

Full Length Article

Substrate induced reconstruction and activation of platinum clusters: A systematic DFT study



Sandeep Nigam*, Chiranjib Majumder

Chemistry Division, Bhabha Atomic Research Centre, Mumbai, 400094, India

ARTICLE INFO

Article history:

Received 15 March 2017

Received in revised form 27 May 2017

Accepted 4 June 2017

Available online 9 June 2017

Keywords:

Pt-Cluster

Al-terminated Al_2O_3 -surface

DFT

Effect of support

ABSTRACT

The fundamental understanding of the electronic and geometric structures of small platinum clusters on metal oxide support is important to design the futuristic Pt-based novel materials for heterogeneous catalysis. Here we report a systematic theoretical study on the trend in the structural and electronic properties of alumina supported Pt_n ($n = 1-7$ and 10) clusters with a focus to highlight the effect on the substrate. All calculations were carried out using the plane wave based pseudo-potential approach. The model for the support has been designed by using Al-terminated $\alpha\text{-Al}_2\text{O}_3$ (0001) surface which is the most stable surface termination under ultrahigh vacuum conditions. The results show that the binding of Pt atom with the Al_2O_3 surface releases 1.84 eV energy which is significantly higher than atomic adsorption energy of other noble metal atoms (Ag, Au, and Pd). As a consequence, the equilibrium geometries of free Pt_n clusters ($n = 3-7$) are significantly altered on the alumina surface. Whilst Pt_{10} cluster favors tetracapped prism structure in the gas phase, on alumina support it prefers a layered structure. The geometrical changes of Pt clusters on the alumina surface have been attributed to the energy balance between the Pt-Pt and Pt-substrate interactions. The nature of interaction between the Pt_n clusters and surface has been verified using the electronic density of states analysis. Surface induced electronic charge on the deposited cluster results in red shift in its energy levels, indicating electron rich activation of platinum clusters. The inclusion of spin-orbit coupling (SOC) significantly changes the electronic structure of gas phase platinum cluster; however, the extent of SOC influence reduces due to interfacial bonding with alumina support.

© 2017 Elsevier B.V. All rights reserved.

1. Introduction

During the past decade, study of deposited clusters has gained significant momentum due to their applications in the field of nano-catalysis. Noble metal clusters supported on oxide support have shown potential for low temperature oxidation catalyst [1,2]. This has prompted researchers to investigate the growth pattern of cluster on oxide support to get insight about the cluster substrate interaction. Various experimental and computational studies have reported that cluster-support interactions result in modified geometry and electronic structure of deposited clusters, leading to novel physico-chemical properties [3–21].

In the periodic table, platinum is known to be the most sought-after element for its applications in the field of homo and heterogeneous catalysis. Platinum clusters have been extensively

used as a catalyst for many reactions viz., oxidation of CO and other hydrocarbons [22,23], water gas shift [24], H_2 dissociation [25], oxygen reduction in fuel cells [26]. Platinum nano-particles have been used in catalytic converters to reduce toxic pollutants such as CO, NO_x , and hydrocarbons [27–30]. In particular, study of chemical reactions on supported Pt clusters has remained as one of the thrust areas of research. This is because of the influence of a substrate which helps in changing the electronic structure and chemical reactivity of the deposited platinum clusters. Previously several studies attempted to understand the growth of Pt nanoclusters on various supports; such as MoS_2 surface [30], $\gamma\text{-Al}_2\text{O}_3$ surface [31], anatase $\text{TiO}_2(101)$ surface [32–34], rutile $\text{TiO}_2(110)$ surface [35,36], graphene [37–40], ceria $\text{CeO}_2(111)$ surface [41], h-BN surface [42] and $\alpha\text{-Al}_2\text{O}_3$ surface [43,44]. Saidi et al. reported the atomic structure of supported Pt_n ($n \leq 12$) clusters on $\text{MoS}_2(001)$ surface using the DFT approach [30]. The results revealed that for $n < 5$, the equilibrium geometry adopts planar configurations. For $n \geq 5$, the Pt_n clusters prefer non-planar 3D configurations as the lowest energy structure. Musgrave and coworkers [34] studied the growth of Pt_n ($n \leq 37$) clusters on the defect-free TiO_2 anatase (101)

* Corresponding author.

E-mail addresses: snigam@barc.gov.in, snigam.jpr@gmail.com (S. Nigam), chiranjib@barc.gov.in (C. Majumder).

surface using DFT pseudo-potential calculations and showed that formation of island-like particles is favored over planar monolayers. Further they verified the DFT results with experiments using atomic layer deposition of Pt atoms and high-resolution transmission electron microscopy. Jiang et al. [36] calculated the optimized geometries of Pt_n ($n = 4-8$) clusters on rutile $TiO_2(110)$ surface. They reported that while tetramer Pt_4 cluster prefers a nearly flat square structure, larger clusters such as Pt_5 , Pt_6 , Pt_7 , and Pt_8 have bi-layer structure with the top layer not interacting with the support directly.

The study of Pt clusters on alumina support is of special importance because both Pt and Al_2O_3 are key materials in conventional automotive exhaust catalysts. Watanabe and co-workers [43] investigated the size-selected Pt_n clusters ($n = 7-20$) on NiAl supported Al_2O_3 film using different experimental techniques such as scanning tunneling microscopy (STM), infrared reflection absorption spectroscopy (IRAS), and temperature-programmed desorption (TPD) study. They reported that Pt_n clusters adsorbed flat on the surface with a planar structure up to $n = 18$ and three dimensional (3D) bi-layer structures starts appearing from $n = 19$ onwards. As the preference of cluster geometry on a surface would depend on a delicate energy balance between metal-metal and metal-substrate interactions, generalization of the cluster growth model on support remained unsolved and challenging issue. Zhou et al. [44] theoretically studied the interaction of platinum clusters Pt_n ($n = 1-5$) with $\alpha-Al_2O_3(0001)$ surface. In this context, it is worth mentioning that they have carried out their investigations on the O-terminated surface where the Al and O atoms of the top layer are arranged in zig-zag manner. However, various experimental [45–50] and theoretical investigations [51–55] have established that Al-terminated $\alpha-Al_2O_3(0001)$ is the most stable surface termination under ultrahigh vacuum conditions. Moreover, because of strong metal oxygen bond, the O-terminated surface is ought to give higher and overestimated adsorption energy. Therefore, so far most of the studies on $\alpha-Al_2O_3(0001)$ surface has been carried out using Al-termination [13–15,56–58]. Even for rationalization of experimental results, the energetics of Al-terminated surface has been considered for comparison [43]. Further, it is also well established that after relaxation of $\alpha-Al_2O_3(0001)$ bulk cut surface, the top Al and O atoms becomes almost co-planar [48–50,56–58], giving equal opportunity for both Al and O to interact with the incoming adsorbate atom. Therefore, Al-terminated $\alpha-Al_2O_3(0001)$ surface is more appropriate (in comparison to zig-zag O-terminated $\alpha-Al_2O_3(0001)$ surface) for correctly portrait the adhesion behavior of the deposited metal clusters.

Motivated by above studies, in the present work, we have carried out a systematic theoretical study of the structural and electronic properties of supported $Pt_n@Al_2O_3$ ($n = 1-7, 10$) clusters with an aim to understand the various factors involved in the evolution of platinum clusters on alumina substrate (viz. cluster geometry, charge distribution at the cluster substrate interface, electronic structure, etc.). To get correct representation of the surface, Al-terminated and fully relaxed $\alpha-Al_2O_3(0001)$ has been used as model substrate. In order to get an insight into the effect of surface morphology, the result of deposited platinum clusters is compared with those of bare gas phase cluster. Present work aims to answer few particular questions such as; (i) how the geometry of a gas phase platinum cluster gets affected upon interaction with a surface? (ii) What is the effect of substrate morphology (termination) on the electronic structure of platinum clusters after deposition? Compare the results obtained on Al-terminated $\alpha-Al_2O_3(0001)$ surface with the previously reported one on O-terminated $\alpha-Al_2O_3(0001)$ surface [44]. (iii) What is the nature of bonding at the interface? (iii) Is there any effect of spin orbit coupling (SOC) on bonding and energetics? Outcome of the present work is expected to provide a connecting

link between different competing factors responsible for the change in the physico-chemical behavior of supported platinum clusters.

2. Computational details

Plane wave based pseudo-potential method as implemented in the Vienna *ab initio* Simulation Package (VASP) [59–61] has been used in all the calculations done in the present work. Full-potential all-electron projector augmented wave (PAW) method [62], as employed in VASP [63] has been used to describe electron-ion interaction. Scalar relativistic corrections were included in generation of PAW pseudo-potential. Exchange correlation energy has been estimated by spin polarized form of GGA [64]. After the spin polarized calculations, the obtained structures were re-optimized by including spin orbit coupling. Plane wave basis set cut off energy was 400 eV. The geometry optimization was done under conjugate gradient formalism with convergence criterion for the forces as 0.01 eV/Å or less. Gas-phase cluster calculations were done by using simulation cell of size $15 \times 15 \times 15$ Å to avoid any kind of image interaction. For deposited platinum cluster 2×2 supercell of alumina substrate having 120 atoms with dimensions $9.53 \times 9.53 \times 25.99$ Å were used. For deposition of Pt_{10} cluster, 3×3 supercell with $14.30 \times 14.30 \times 25.99$ Å dimension as (surface area ≈ 204.4 Å²) and containing 270 atoms have been used. Other calculation parameters and computational procedures has been kept same as reported in our previous work [15]. To get the ground state isomer of platinum cluster on alumina substrate, various possible adsorption sites have been identified. For convenient reading and easy visualization, we have labeled each adsorption site with a letter and a number indicating the type of the atom and the atomic layer in the slab, respectively i.e. Al(1), O(2), Al(3), Al(4), and O(5) as presented in Fig. S1 of Supporting information. The average adsorption energy of Pt_n cluster on $\alpha-Al_2O_3$ surface was calculated as $\Delta E = [E(Pt_n/Al_2O_3) - E(Al_2O_3) - E(Pt_n)]/n$.

3. Result and discussion

To start with, the equilibrium geometries of the free Pt_n cluster ($n = 1-7, 10$) were optimized. The effect of the spin-orbit-coupling interactions on these clusters was realized by calculating the total energies with and without SOC terms. The results showed preference of planar geometries for small Pt_n ($n = 2-7$) clusters, which are in line with the results reported earlier [65]. Inclusion of the spin orbit coupling term in the total energy calculation did not influence the ground state geometries significantly albeit the binding energy for smaller size clusters reduces. For Pt_{10} cluster, the lowest energy isomer forms a three-dimensional tetracapped prism structure as shown in Fig. 1. After probing the structure and energetics of the gas phase clusters, we have systematically investigated the adsorption of these clusters on the $\alpha-Al_2O_3(0001)$ surface.

To locate the most preferred adsorption site of Pt atom on the $\alpha-Al_2O_3(0001)$ surface several configurations were optimized by placing the Pt atom on various well-defined adsorption sites; (i) on top of the Al atom of top most layer of surface (ii) on top of the O atom of second layer (iii) by capping the Al–O bond of the surface in bridging mode. On the basis of the total energy for all optimized geometries it is seen that Pt prefers to bind with surface Al atom at a tilted angle ($\sim 55^\circ$) with respect to the surface plane. The binding energy of Pt atom by non-spin orbit coupling calculation is 2.06 eV. The shortest Pt–Al bond distance is ~ 2.35 Å. Moreover, during the process of Pt adsorption, the surface Al atom, which is otherwise co-planar with surface O-atoms, moves upward by 0.42 Å. This can be viewed as reverse relaxation of surface Al atoms. After inclusion of SOC term in total energy calculation, the adsorption energy of Pt atom on surface reduces to 1.84 eV. It is worth mentioning

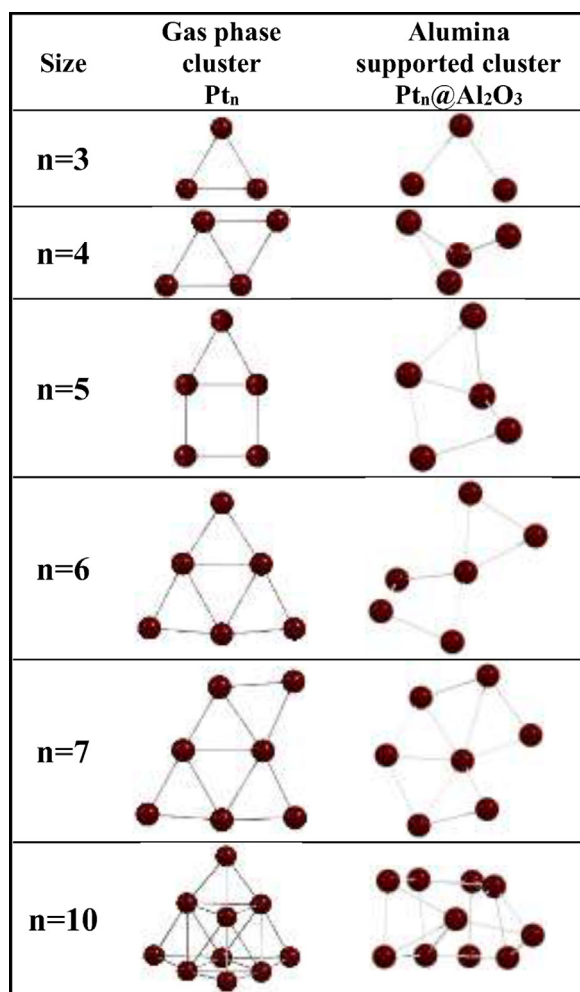


Fig. 1. Optimized structures of gas phase and alumina supported platinum clusters. For clarity and better visualization alumina support has not been shown here.

that Zhou and co-workers [44] reported the adsorption energy of Platinum as 7.70 eV on an unrelaxed O-terminated α - Al_2O_3 (0001) surface (zig-zag top layers of Al and O) by non-spin orbit coupling calculations. Further because of zig-zag nature of the substrate, the surface reconstruction (upwards movement of Al atom) was also not reported by them. A comparison of the binding strength among other noble metals (Ag, Au, and Pd) suggest stronger binding for Pt atoms [13–15], indicating stronger cohesion between adatom (Pt) and the substrate (Al_2O_3). The results for other Pt clusters are described through following sections. The geometry of the lowest energy isomers of $Pt_n@Al_2O_3$ clusters has been compared with corresponding gas phase cluster in Fig. 1. Top and side view of composite system and other parameters like bader charge and energetics are presented in the Fig. S2 and Table S1 of Supporting information, respectively. Other low lying isomers of $Pt_n@Al_2O_3$ are presented in Fig. 2.

The adsorption of Pt_2 dimer on the Al_2O_3 surface can provide the information regarding the energy economy between Pt–Pt and Pt–substrate interaction. To obtain the most favorable structure of Pt_2 dimer on the alumina surface two configurational methodologies have been adopted; (i) Placement of Pt_2 dimer in parallel and perpendicular fashion on the surface at various angles and (ii) two Pt atoms are placed at a distance of 4–5 Å on the surface. Based on the total energy consideration, it is seen that when Pt_2 dimer is placed at an angle (tilt) to the surface that forms the lowest energy

configuration as shown in Fig. 2. Here one Pt is bound with one of the Al atoms at the top layer and the other Pt atom moves upward projecting on the bridge site of the Al–O (second layer) bond. The Pt–Al, Pt–Pt and Pt–O bond lengths are found to be 2.46–2.65 Å, 2.44 Å, and 2.01–2.02 Å, respectively. We note that the Pt–Pt bond (2.38 Å) in the free cluster is elongated (2.44 Å) marginally upon deposition. Moreover, Pt_2 induces structural relaxation (local) in the alumina surface. In particular the Al atom, which is connected to the Pt, moves upward by 0.4 Å from the surface plane. The adsorption energy of Pt_2 is found to be 1.17 eV/atom. For the second case, where two Pt atoms are placed far (4–5 Å) away and optimize the atomic positions of all atoms they do not coalesce each other to form Pt_2 dimer. Also, from the energy point of view this adsorption mode (atomic) is unfavorable by 2.11 eV than the dimer structure. The lower stability of the atomic adsorption mode is ascribed to absence of strong Pt–Pt bond. Therefore, it is inferred that for Pt adsorption, clustering of atoms through Pt–Pt bonds is more favorable in comparison to isolated attachment of Pt atom on alumina surface. However, a kinetic barrier always will be there between the two said configurations. It needs to be mentioned that contrary to the present results, Zhou and co-workers [44] reported that on O-terminated Al_2O_3 surface, the atomic adsorption mode is favorable (adsorption energy 9.08 eV/atom) in comparison to the dimer adsorption (adsorption energy 5.53 eV/atom). The difference in the adsorption behavior is due to two factors; (i) the clean O-terminated Al_2O_3 surface was unrelaxed and (ii) the larger strength of the Pt–O than Pt–Al bond. Moreover, as Pt–O bond is much stronger than Pt–Al and Pt–Pt bond, the Pt atom adsorption lead to much higher binding energy and favors the dissociation of Pt atoms.

To get the ground state geometry of Pt_n ($n=3-7$) clusters on alumina support two approaches were adopted (i) The gas phase structure of Pt_n cluster was placed in different orientations (parallel, perpendicular and tilted to the surface) at various possible sites of Al_2O_3 surface (ii) addition of Pt atom on the most stable geometry of the Pt_{n-1} clusters deposited on the Al_2O_3 surface followed by subsequent optimization. For Pt_3 it is seen that the close triangular structure of the gas phase trimer becomes an open structure on the Al_2O_3 surface, where two Pt atoms are bound with two surface Al atoms and the central Pt atom is tilted towards surface O atom, as shown in Fig. 2. The Pt–Pt distance and Pt–Pt–Pt angle are found to be 2.47 Å and 67.4°, respectively. As two Pt atoms are connected to the Al atoms of the top layer, two Al atoms are moved out of plane by about 0.35 Å. The binding energy of the Pt_3 cluster on the Al_2O_3 surface is estimated to be 1.07 eV/atom. The Pt_3 cluster placed vertically on the Al_2O_3 surface is 0.3 eV higher in energy as compared to the lowest energy isomer. Zhou and co-workers [44] reported equilateral triangle Pt_3 on O-terminated Al_2O_3 surface, with adsorption energy as 4.27 eV/atom.

Tetramer cluster are interesting as $n=4$, is the smallest size for a cluster which can adopt three dimensional configurations. The ground state geometry of the free Pt_4 cluster is planar rhombus. In order to identify the equilibrium geometry of the tetramer Pt_4 cluster on the alumina surface we have optimized several configurations. A comparison of the total energy of different optimized structures suggests that a bent rhombus configuration of the Pt_4 cluster is the lowest energy isomer. The Pt–Al distances are found to be 2.46 Å. The Pt–Pt distances are found to be 2.50, 2.57 Å. The binding energy of Pt_4 cluster on the Al_2O_3 surface is found to be 0.94 eV/atom. Contrary to this, Zhou and co-workers [44] have reported that on O-terminated Al_2O_3 surface, Pt_4 prefers a highly distorted or in other words dissociated rhombus structure (rhombus cluster is decomposed into an equilateral triangle and an isolated atom) with adsorption energy as 3.99 eV/atom.

The edge capped rhombus structure of Pt_5 cluster, which is the lowest energy configuration in the gas phase, is distorted upon

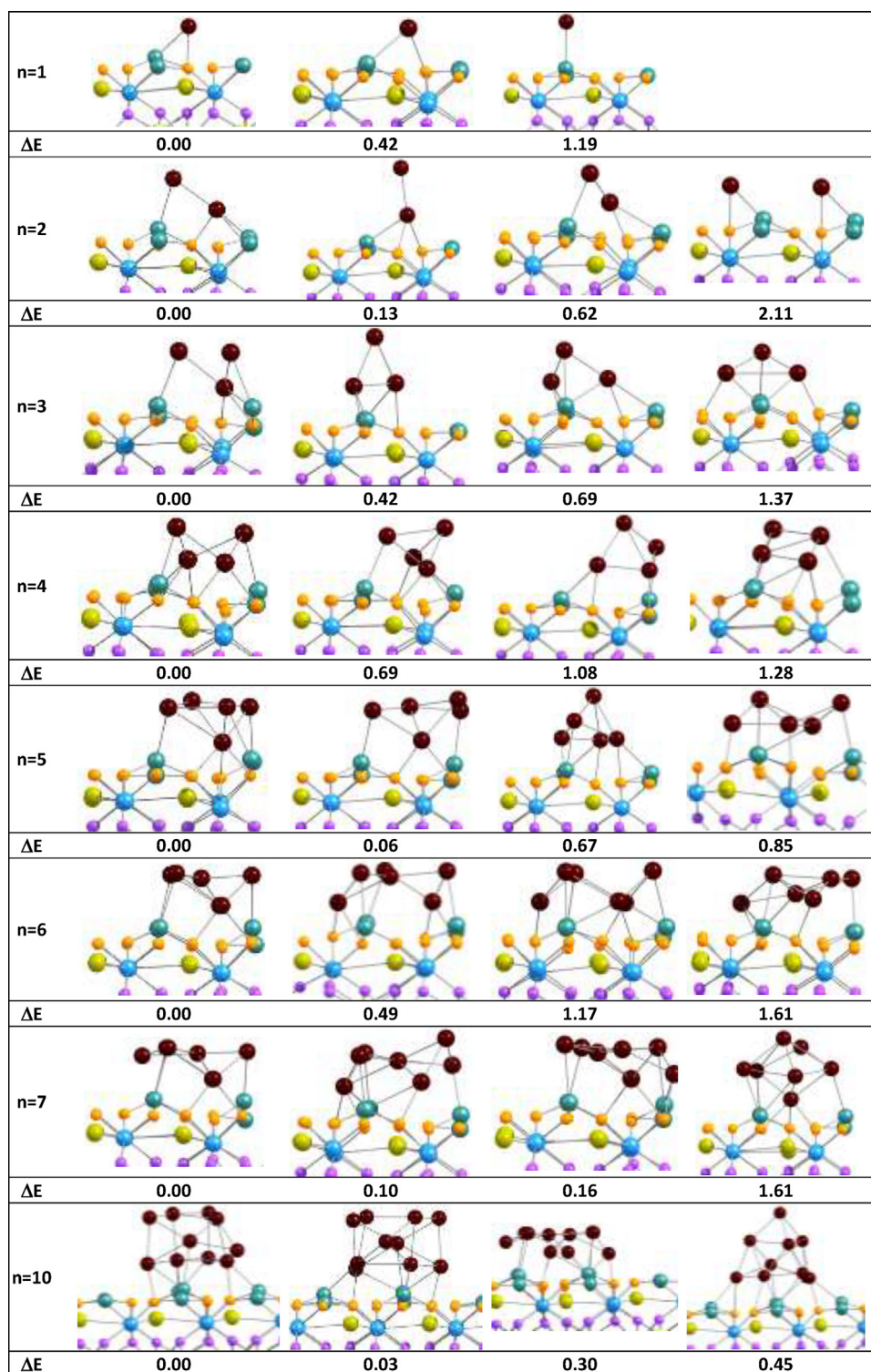


Fig. 2. Low lying isomers of $Pt_n@Al_2O_3$ clusters with decreasing relative stability (ΔE eV).

interaction with the Al_2O_3 surface. The optimized geometry of the Pt_5 cluster on the Al_2O_3 surface forms capped bent rhombus as shown in Figs. 1 and 2. Three Pt atoms are bonded to top Al atoms and other two occupy the hollow site. The average Pt–Al and Pt–Pt bond lengths are found to be 2.52 Å, and ~2.5 Å respectively. The binding energy of Pt_5 on the Al_2O_3 surface is estimated to be 0.73 eV/atom. Zhou and co-worker [44] reported square pyramidal structure of Pt_5 on O-terminated Al_2O_3 surface, with adsorption energy as 3.12 eV/atom.

Gas phase triangular Pt_6 cluster is small cut of Pt (111) surface. The most stable geometry of the Pt_6 cluster on the Al_2O_3 surface adopts configuration having a dimer plus tetramer joined on the surface. The average Pt–Al and Pt–Pt bond lengths are found to be 2.45 Å, and ~2.6 Å respectively. The binding strength of Pt_6 on Al_2O_3 is 0.70 eV/atom. The triangular and hexagonal isomer of Pt_6 are 0.5 and 1.2 eV higher in energy respectively. The gas phase structure of Pt_7 cluster is capped planar triangle which is also looks like a small cut of the truncated Pt(111) surface. Upon optimization of

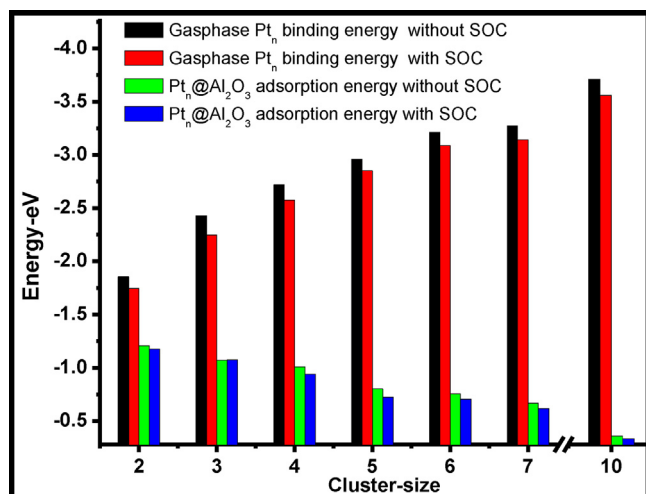


Fig. 3. Variation in average binding energy of gas phase Pt_n cluster and average adsorption energy of Pt_n cluster on alumina substrate with cluster size.

several configuration of Pt₇ cluster on the Al₂O₃ surface, the lowest energy isomer obtained is a zig-zag pseudo hexagonal structure with six platinum atoms arranged in up and down fashion. While the 'up' platinum atoms bind with top layer Al atoms, the 'down' atoms occupy the hollow site Al(4) and the central Pt atom occupies the Al(3) hollow site. This structure resembles with hexagonal pattern but one of the edges of the hexagon (Pt-Pt) is elongated upto 3.79 Å. The adsorption energy of the Pt₇ on alumina is found to be 0.64 eV/atom.

The Pt₁₀ cluster shows drastic modification on deposition on alumina substrate as it forms bilayer structure with adsorption energy as 0.33 eV/atom. The planar zig-zag isomer is 0.58 eV higher in energy. Tetracapped prism structure which is lowest energy structure in the gas phase, on deposition, it is found to be 0.89 eV higher in energy in comparison to ground state isomer. Thus, based on the above results, it is clear that, gas phase geometry of platinum clusters gets modified on alumina support. This modification leads to 2–3% increase in the average Pt–Pt bond length. The energy balance between the Pt – substrate and Pt-Pt interactions gives the final adsorption energy of Pt_n@Al₂O₃ cluster. Fig. 3 shows the variation in average binding energy of isolated clusters along with their average adsorption energy as a function of cluster size. In general, the average binding energy of gas phase Pt clusters increases smoothly as a function of cluster size. On the contrary, average adsorption energy of Pt clusters on the alumina surface decreases with cluster size. Importantly, the trend remains similar irrespective of the inclusion of SOC term in the total energy calculations. For the gas phase cluster, the spin orbit coupling changes the binding energies values by ~0.14 eV, while for deposited platinum clusters the adsorption energy values changes by ~0.04 eV. Thus, inclusion of spin orbit coupling has lesser influence on energetics of the supported clusters than the gas phase platinum clusters. Further it is important to note that adsorption energies of platinum clusters previously reported [44] on O-terminated α-Al₂O₃ (0001) surface are much higher than the corresponding adsorption energies on Al-terminated α-Al₂O₃ (0001) surface presented in current work.

In order to have qualitative understanding of the nature of bonding at the cluster-surface interface, charge difference analysis has been carried out. The charge density difference at the interface of Pt cluster and alumina surface is calculated as

$$\Delta\rho = \rho(\text{Pt}_n/\text{Al}_2\text{O}_3) - \rho(\text{Al}_2\text{O}_3)_{\text{fix}} - \rho(\text{Pt}_n)$$

where $\rho(\text{Pt}_n/\text{Al}_2\text{O}_3)$ is the charge density of the total system, $\rho(\text{Al}_2\text{O}_3)_{\text{fix}}$ is the charge density of the clean alumina surface, and

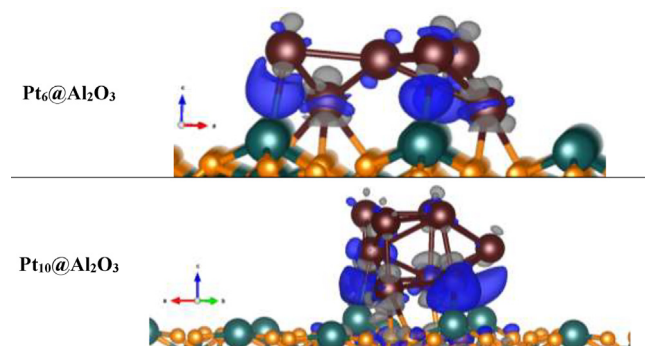


Fig. 4. The charge density difference ($\Delta\rho$) of supported Pt_n cluster. Blue shows an increase in the charge density, and gray shows a decrease in the charge density. (For interpretation of the references to colour in this figure, the reader is referred to the web version of this article.)

$\rho(\text{Pt}_n)$ is the electron density of the isolated cluster. The results show that an overall charge transfer happens from alumina surface to the Pt cluster. Fig. 4 depicts two representative charge density difference contours for Pt₆ and Pt₁₀ clusters on the Al₂O₃ surface. Bader analysis was carried out to quantify the atomic charge distribution. It is found that Pt_n clusters acquire considerable electronic charge from the Al₂O₃ surface. In case of Pt atom deposited on the Al₂O₃ surface, where Pt atom binds with one of the surface Al atoms, Pt gains partial negative charge of about 0.37e. Bader analysis shows that an accumulation of 0.56e, 0.78e, 0.90 and 1.12e charge on the Pt₂, Pt₃, Pt₄ and Pt₅ cluster respectively. Charge accumulation and depletion was observed on the alternate Pt atoms of the Pt₆ cluster, with an overall charge gain of 1.2e. For Pt₇ cluster also 1.23e charge was gained from the surface. However, for Pt₁₀ cluster the amount of charge gained by cluster reduces to 1.15e. This is due to the fact that the deposited Pt₁₀ cluster forms bilayer structure. Here lesser number of Pt atoms are interacting with the surface. The opposite trend in the adsorption energy of Pt clusters and gas-phase binding energy can also be explained by considering large charge transfer at the interface between Pt clusters and Al₂O₃ surface.

To get the deeper insight about the interface bonding, electronic structure of all Pt_n clusters was analyzed before and after the adsorption on the Al₂O₃ substrate. Importantly, the effect of SOC on the electronic structure of gas phase Pt clusters was found to be significant (Figs. S3–S4 of Supporting information). Inclusion of spin orbit coupling leads to more hybridization among *spd* orbitals. In the case of deposited clusters, we have plotted the density of states (DOS) of Pt_n clusters before and after deposition on the Al₂O₃ surface. Projected DOS analysis on the platinum atomic orbitals is shown in Fig. 5 by taking Pt₁₀ as representative example. This was prepared and analyzed by separating out the contributions from the adsorbed Pt_n clusters and the Al₂O₃ surface to the total-DOS of the system. The projected DOS of all clusters is presented in the Fig. S5 of Supporting information. A significant red shift in the electronic states of the Pt_n clusters is observed upon adsorption of Pt_n on the Al₂O₃ substrate. This indicates activation of platinum clusters by the support. This is in accordance with the excess electronic charge accumulation on the deposited Pt atoms, which destabilizes the energy levels to the higher side (less negative energy) with increase in hybridization and broadening. It is also important to note that the Fermi energy level of the Al₂O₃ – Pt_n system is less negative as compared to the clean Al₂O₃ and Pt_n components. This corroborates the electronic charge transfer from the surface to the platinum clusters. Furthermore, it is seen that the Fermi energy level is predominantly contributed by the atomic orbitals from Pt atoms. Further we note that as more and more Pt atoms become connected with the surface, the effect of SOC on the electronic structure reduces. This can

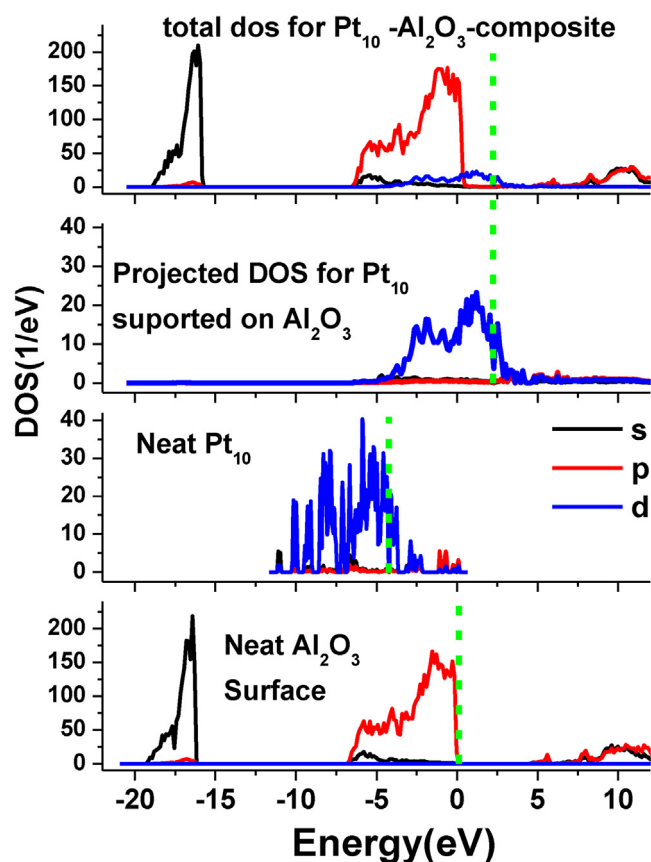


Fig. 5. Comparative density of states (DOS) for Pt₁₀ cluster before and after deposition on alumina substrate. Vertical dotted line indicates the Fermi level.

be corroborated by comparing the effect of SOC on electronic structure of gas phase and supported Pt_n cluster as presented in Figs. S3–S4 of Supporting information. As clear from Fig. S4, platinum d-orbital in the gas phase Pt_n cluster has greater influence of SOC in comparison to corresponding supported cluster. This is understandable as more and more number of platinum atoms will be getting connected to the surface Al/O atoms, more overlap between localized *p*-orbital of surface and *d*-orbital of adsorbate cluster will occur, leading to weakening of the SOC effect. These results are in line with the observed energetics of platinum cluster, where it is found that inclusion of spin orbit coupling has more influence on energetic values of gas phase clusters in comparison to supported platinum clusters.

4. Conclusions

In summary, we have presented the structure and electronic properties of small Pt clusters on clean and relaxed Al-terminated α -Al₂O₃ (0001) surface. All calculations were carried out using first principles method under the formalism of spin polarized density functional theory. A comparison in the structure and energetics of platinum clusters between the Al-terminated and O-terminated α -Al₂O₃ (0001) surface reveals the importance of surface morphology of the support as both termination have different structure and energetics. The binding energy of single Pt atom on Al-terminated alumina surface is 1.84 eV. In fact, a comparison of this result with other noble metal atoms (Ag, Au, Pd) suggests that binding strength of Pt is significantly stronger than others. In general, the ground state geometry of the supported Pt_n cluster is different from the gas phase. On the support the Pt clusters preferentially adsorb parallel to the surface plane by placing the alternate Pt atoms up and

down fashion, forming a quasi-planar structure. In case of Pt₁₀, bilayer structure forms the lowest energy isomer on the alumina surface. This is different than the gas phase equilibrium structure of Pt₁₀ cluster, which adopts tetracapped prism shape. Both Pt–Pt and Pt–surface interactions are strong and therefore, a balance of energetics between them decides the lowest energy structure of the composite system. It is found that spin-orbit coupling (SOC) has significant effect on the electronic structure of bare platinum cluster, but the impact of SOC reduces for the supported cluster due to interfacial bonding with the surface. The charge distribution analysis shows transfer of electronic charge from surface to the adsorbed Pt cluster. Injection of charge into platinum cluster leads a red shift in the energy levels as reflected in the density of states spectrum. This is an indication for enhanced chemical reactivity. Since Al-terminated α -Al₂O₃ (0001) is reported to be the most stable surface termination, we believe that our results will be more suitable for interpretation of the experimental results.

Acknowledgement

We are thankful to the members of the Computer Division, BARC, for their kind cooperation during this work.

Appendix A. Supplementary data

Supplementary data associated with this article can be found, in the online version, at <http://dx.doi.org/10.1016/j.apsusc.2017.06.041>.

References

- [1] D.W. Goodman, Model studies in catalysis using surface science probes, *Chem. Rev.* 95 (1995) 523–536.
- [2] B.C. Gates, Supported metal clusters: synthesis, structure, and catalysis, *Chem. Rev.* 95 (1995) 511–522.
- [3] M. Haruta, Gold as a novel catalyst in the 21st century: preparation working mechanism and applications, *Gold Bull. (Lond.)* 37 (2004) 27–36.
- [4] M. Valden, X. Lai, D.W. Goodman, Onset of catalytic activity of gold clusters on titania with the appearance of nonmetallic properties, *Science* 281 (1998) 1647–1650.
- [5] B. Yoon, H. Hakkinen, U. Landman, A.S. Wörz, J.-M. Antonietti, S. Abbet, K. Judai, U. Heiz, Charging effects on bonding and catalyzed oxidation of CO on Au₈ clusters on MgO, *Science* 307 (2005) 403–407.
- [6] A. Bongiorno, U. Landman, Water-enhanced catalysis of CO oxidation on free and supported gold nanoclusters, *Phys. Rev. Lett.* 95 (2005) 106102.
- [7] Y. Lei, F. Mehmood, S. Lee, J. Greeley, B. Lee, S. Seifert, R.E. Winans, J.W. Elam, R.J. Meyer, P.C. Redfern, D. Teschner, R. Schlögl, M.J. Pellin, L.A. Curtiss, S. Vajda, Increased silver activity for direct propylene epoxidation via subnanometer size effects, *Science* 328 (2010) 224–228.
- [8] L. Cheng, C. Yin, F. Mehmood, B. Liu, J. Greeley, S. Lee, B. Lee, S. Seifert, R.E. Winans, D. Teschner, R. Schlögl, S. Vajda, L.A. Curtiss, Reaction mechanism for direct propylene epoxidation by alumina-supported silver aggregates: the role of the particle/support interface, *ACS Catal.* 4 (1) (2014) 32–39.
- [9] C. Yin, E. Tyo, K. Kuchta, B. von Issendorff, S. Vajda, Atomically precise (catalytic) particles synthesized by a novel cluster deposition instrument, *J. Chem. Phys.* 140 (2014) 174201.
- [10] G. Barcaro, L. Sementa, F.R. Negreiros, R. Ferrando, A. Fortunelli, Interface effects on the magnetism of CoPt-supported nanostructures, *Nano Lett.* 11 (2011) 5542–5547.
- [11] S. Surnev, A. Fortunelli, F.P. Netzer, Structure-property relationship and chemical aspects of oxide-metal hybrid nanostructures, *Chem. Rev.* 113 (2013) 4314–4372.
- [12] R. Ferrando, G. Barcaro, A. Fortunelli, Structures of small Au clusters on MgO(001) studied by density-functional calculations, *Phys. Rev. B* 83 (2011) 045418.
- [13] S. Nigam, C. Majumder, Growth pattern of Ag_n (n = 1–8) clusters on the α -Al₂O₃ (0001) surface: a first principles study, *Langmuir* 26 (2010) 18776–18787.
- [14] S. Nigam, C. Majumder, Adsorption of small palladium clusters on the α -Al₂O₃ (0001) surface: a first principles study, *J. Phys. Chem. C* 116 (2012) 2863–2871.
- [15] C. Rajesh, S. Nigam, C. Majumder, The structural and electronic properties of Au_n clusters on the α -Al₂O₃ (0001) surface: a first principles study, *Phys. Chem. Chem. Phys.* 16 (2014) 26561–26569.
- [16] G. Pacchioni, Electronic interactions and charge transfers of metal atoms and clusters on oxide surfaces, *Phys. Chem. Chem. Phys.* 15 (2013) 1737–1757.

- [17] N.C. Hernandez, J.F. Sanz, First principles simulations of Cu and Au deposition on α -Al₂O₃ (0001) surface, *Appl. Surf. Sci.* 238 (2004) 228–232.
- [18] J.J. Plata, J. Graciani, J. Evans, J.A. Rodriguez, J.F. Sanz, Cu deposited on CeO_x-modified TiO₂ (110): synergistic effects at the metal–oxide interface and the mechanism of the WGS reaction, *ACS Catal.* 6 (7) (2016) 4608–4615.
- [19] A.S. Crampton, M.D. Rötzer, C.J. Ridge, B. Yoon, F.F. Schweinberger, U. Landman, U. Heiz, Assessing the concept of structure sensitivity or insensitivity for sub-nanometer catalyst materials, *Surf. Sci.* 652 (2016) 7–19.
- [20] N. Umezawa, H.H. Kristoffersen, L.B. Vilhelmsen, B. Hammer, Reduction of CO₂ with water on Pt-loaded rutile TiO₂ (110) modeled with density functional theory, *J. Phys. Chem. C* 120 (2016) 9160–9164.
- [21] L. Xiao, W.F. Schneider, Surface termination effects on metal atom adsorption on α -alumina, *Surf. Sci.* 602 (2008) 3445–3453.
- [22] H. Hirata, K. Kishita, Y. Nagai, K. Dohmae, H. Shinjoh, S. Matsumoto, Characterization and dynamic behavior of precious metals in automotive exhaust gas purification catalysts, *Catal. Today* 164 (2011) 467–473.
- [23] A. Siani, K.R. Wigal, O.S. Alexeev, M.D. Amiridis, Synthesis and characterization of γ -Al₂O₃-supported Pt catalysts from Pt₄ and Pt₆ clusters formed in aqueous solutions, *J. Catal.* 257 (2008) 16–22.
- [24] Q. Fu, H. Saltsburg, M. Flytzani-Stephanopoulos, Active nonmetallic Au and Pt species on ceria-based water-gas shift, *Catal. Sci.* 301 (2003) 935–938.
- [25] A. Kaldor, D.M. Cox, Hydrogen chemisorption on gas-phase transition-metal clusters, *Faraday Trans.* 86 (1990) 2459–2463.
- [26] M. Vidotti, V.R. Goncalves, V.S. Quartero, B. Danc, S.I.C. de Torresi, Platinum nanoparticle-modified electrodes, morphologic, and electrochemical studies concerning electroactive materials deposition, *J. Solid State Electrochem.* 14 (2010) 675–679.
- [27] K. Yamamoto, T. Imaoka, W.-J. Chun, O. Enoki, H. Katoh, M. Takenaga, A. Sonoi, Size-specific catalytic activity of platinum clusters enhances oxygen reduction reactions, *Nat. Chem.* 1 (2009) 397–402.
- [28] W. Shieber, H. Vinek, A. Jentys, Oxidation state of platinum clusters during the reduction of NO_x with propene and propane, *Catal. Lett.* 73 (2001) 67–72.
- [29] Y. Shi, K.M. Ervin, Catalytic oxidation of carbon monoxide by platinum cluster anions, *J. Chem. Phys.* 108 (1998) 1757.
- [30] W.A. Saidi, Density functional theory study of nucleation and growth of Pt nanoparticles on MoS₂(001) surface, *Cryst. Growth Des.* 15 (2015) 642–652.
- [31] R.L. Arevalo, H. Kishi, A.A.B. Padama, J.L.V. Moreno, H. Kasai, Substrate dependence of Pt₄ electronic properties, *J. Phys.: Condens Matter* 25 (2013) 222001 (4pp).
- [32] Y. Han, C.-j. Liu, Q. Ge, Interaction of Pt clusters with the anatase TiO₂(101) surface: a first principles study, *J. Phys. Chem. B* 110 (2006) 7463–7472.
- [33] X.-Q. Gong, A. Selloni, O. Dulub, P. Jacobson, U. Diebold, Small Au and Pt clusters at the anatase TiO₂(101) surface: behavior at terraces, steps, and surface oxygen vacancies, *J. Am. Chem. Soc.* 130 (2008) 370–381.
- [34] Y. Zhou, C.L. Muhich, B.T. Neltner, A.W. Weimer, C.B. Musgrave, Growth of Pt particles on the anatase TiO₂ (101) surface, *J. Phys. Chem. C* 116 (2012) 12114–12123.
- [35] S.C. Ammal, A. Heyden, Nature of Pt_n/TiO₂(110) interface under water-gas shift reaction conditions: a constrained ab initio thermodynamics study, *J. Phys. Chem. C* 115 (2011) 19246–19259.
- [36] D.-e. Jiang, S.H. Overbury, S. Dai, Structures and energetics of Pt clusters on TiO₂: interplay between metal-metal bonds and metal-oxygen bonds, *J. Phys. Chem. C* 116 (2012) 21880–21885.
- [37] Y. Li, W. Gao, L. Ci, C. Wang, P.M. Ajayan, Catalytic performance of Pt nanoparticles on reduced graphene oxide for methanol electro-oxidation, *Carbon* 48 (2010) 1124–1130.
- [38] K. Okazaki-Maeda, Y. Morikawa, S. Tanaka, M. Kohyama, Structures of Pt clusters on graphene by first-principles calculations, *Surf. Sci.* 604 (2010) 144–154.
- [39] J.-D. Qiu, G.-C. Wang, R.-P. Liang, X.-H. Xia, H.-W. Yu, Controllable deposition of platinum nanoparticles on graphene as an electrocatalyst for direct methanol fuel cells, *J. Phys. Chem. C* 115 (2011) 15639–15645.
- [40] D.-H. Lim, J. Wilcox, DFT-based study on oxygen adsorption on defective graphene-supported Pt nanoparticles, *J. Phys. Chem. C* 115 (2011) 22742–22747.
- [41] S. Aranifard, S.C. Ammal, A. Heyden, Nature of Pt_n/CeO₂(111) surface under water-gas shift reaction conditions: a constrained ab initio thermodynamics study, *J. Phys. Chem. C* 116 (2012) 9029–9042.
- [42] D. Xu, Y.-j. Liu, J.-x. Zhao, Q.-h. Cai, X.-z. Wang, Theoretical study of the deposition of Pt clusters on defective hexagonal boron nitride (h-BN) sheets: morphologies, electronic structures, and interactions with O, *J. Phys. Chem. C* 118 (2014) 8868–8876.
- [43] A. Beniya, N. Isomura, H. Hiratab, Y. Watanabe, Morphology and chemical states of size-selected Pt_n clusters on an aluminium oxide film on NiAl(110) Phys. Chem. Chem. Phys. 16 (2014) 26485–26492.
- [44] C. Zhou, J. Wu, T.J.D. Kumar, N. Balakrishnan, R.C. Forrey, H. Cheng, Growth pathway of Pt clusters on α -Al₂O₃ (0001) surface, *J. Phys. Chem. C* 111 (2007) 13786–13793.
- [45] J. Ahn, W. Rabalais, Composition and structure of the Al₂O₃ {0001}(1 × 1) surface, *Surf. Sci.* 388 (1997) 121–131.
- [46] J. Toofan, P.R. Watson, The termination of the α -Al₂O₃ (0001) surface: a LEED crystallography determination, *Surf. Sci.* 401 (1998) 162–172.
- [47] G. Renaud, Oxide surfaces and metal/oxide interfaces studied by grazing incidence X-ray scattering, *Surf. Sci. Rep.* 23 (1998) 1–2.
- [48] C. Verdozzi, D.R. Jennison, P.A. Schultz, M.P. Sears, Sapphire (0001) surface clean and with d-metal overlayers, *Phys. Rev. Lett.* 82 (1999) 799.
- [49] E.A. Soares, M.A. Van Hove, C.F. Walters, K.F. McCarty, Structure of the α -Al₂O₃ (0001) surface from low-energy electron diffraction: Al termination and evidence for anomalously large thermal vibrations, *Phys. Rev. B* 65 (2002) 195405.
- [50] S.L. Tait, L.T. Ngo, Q. Yu, S.C. Fain Jr., C.T. Campbell, Growth and sintering of Pd clusters on α -Al₂O₃(0001), *J. Chem. Phys.* 122 (2005) 064712.
- [51] P.W. Tasker, The stability of ionic crystal surfaces, *J. Phys. C: Solid State Phys* 12 (1979) 4977–4984.
- [52] S. Ciraci, I.P. Batra, Electronic structure of α -alumina and its defect states, *Phys. Rev. B* 28 (1983) 982–992.
- [53] M. Causa, R. Dovesi, C. Pisani, C. Roetti, Ab initio characterization of the (0001) and (101–0) crystal faces of α -alumina, *Surf. Sci.* 215 (1989) 259–271.
- [54] I. Manassidis, M.J. Gillan, Structure and energetics of alumina surfaces calculated from first principles, *J. Am. Ceram. Soc* 77 (1994) 335–338.
- [55] M. Gautier-Soyer, F. Jollet, C. Noguera, Influence of surface relaxation on the electronic states of the α -Al₂O₃ (0001) surface: a self-consistent tight-binding approach, *Surf. Sci.* 352 (1996) 755–759.
- [56] B. Hinnemann, E.A. Carter, Adsorption of Al, O, Hf, Y, Pt, and S atoms on α -Al₂O₃ (0001), *J. Phys. Chem. C* 111 (2007) 7105–7126.
- [57] L.G. Briquet, C.R.A. Catlow, S.A. French, Comparison of the adsorption of Ni, Pd, and Pt on the (0001) surface of α -Alumina, *J. Phys. Chem. C* 112 (2008) 18948–18954.
- [58] C. Rohmann, J.B. Metson, H. Idress, DFT study of carbon monoxide adsorption on α -Al₂O₃ (0001), *Surf. Sci.* 605 (2011) 1694–1703.
- [59] G. Kresse, J. Furthmüller, Efficient iterative schemes for ab initio total-energy calculations using a plane-wave basis set, *Phys. Rev. B* 54 (1996) 11169–11186.
- [60] G. Kresse, J. Furthmüller, Efficiency of ab-initio total energy calculations for metals and semiconductors using a plane-wave basis set, *Comp. Mater. Sci.* 6 (1996) 15–50.
- [61] D. Vanderbilt, Soft self-consistent pseudopotentials in a generalized eigenvalue formalism, *Phys. Rev. B* 41 (1990) 7892–7895.
- [62] P.E. Blochl, Projector augmented-wave method, *Phys. Rev. B* 50 (1994) 17953–17979.
- [63] G. Kresse, D. Joubert, From ultrasoft pseudopotentials to the projector augmented-wave method, *Phys. Rev. B* 59 (1999) 1758–1775.
- [64] J.P. Perdew, J.A. Chevary, S.K. Vosko, K.A. Jackson, M.R. Pederson, D.J. Singh, C. Fiolhais, Atoms, molecules, solids, and surfaces: applications of the generalized gradient approximation for exchange and correlation, *Phys. Rev. B* 46 (1992) 6671–6687.
- [65] K. Bhattacharyya, C. Majumder, Growth pattern and bonding trends in Pt_n (n = 2–13) clusters: theoretical investigation based on first principle calculations, *Chem. Phys. Lett.* 446 (2007) 374–379.